Inorganic Chemistry

Article

pubs.acs.org/IC

A Porous 4-Fold-Interpenetrated Chiral Framework Exhibiting Vapochromism, Single-Crystal-to-Single-Crystal Solvent Exchange, Gas Sorption, and a Poisoning Effect

Ming-Hua Zeng,*[,†] Yan-Xi Tan,[†] Yan-Ping He,[†] Zheng Yin,[†] Qing Chen,[†] and Mohamedally Kurmoo*[,‡]

[†]Key Laboratory for the Chemistry and Molecular Engineering of Medicinal Resources (Ministry of Education), Department of Chemistry and Chemical Engineering, Guangxi Normal University, Guilin 541004, People's Republic of China

[‡]Laboratoire DECOMET, Institut de Chimie de Strasbourg, Université de Strasbourg, CNRS-UMR 7177, 4 rue Blaise Pascal, CS 90032, 67081 Strasbourg Cedex, France

Supporting Information

ABSTRACT: The synthesis and characterization of a 4-fold-interpenetrated pseudodiamond metal−organic framework (MOF), $Co^{II}(pybz)_2 \cdot 2DMF$ [pybz = 4-(4-pyridyl)benzoate], are reported. *N*,*N*-Dimethylformamide (DMF) of the channels can be removed to give the porous framework, and it can also be exchanged for methanol, ethanol, benzene, and cyclohexane. It is a rare example of a stable MOF based on a single octahedral building unit. The single-crystal structures of $Co^{II}(pybz)_2 \cdot 2DMF$, $Co^{II}(pybz)_2$, $Co^{II}(pybz)_2 \cdot 4MeOH$, and $Co^{II}(pybz)_2 \cdot 2.5EtOH$ have been successfully determined. In all of them, the framework is marginally modified and contains a highly distorted and strained octahedral node of cobalt with two pyridine nitrogen atoms and two chelate carboxylate groups. In air, the crystals of $Co^{II}(pybz)_2 \cdot 2DMF$ readily change color from claret red to light pink. Thermogravimetric analysis and Raman spectroscopy indicate a change in coordination, where the carboxylate becomes monodentate and an additional two water molecules are coordinated to each cobalt atom. In a dry solvent, this transformation does not take place. Tests show that $Co^{II}(pybz)_2$ may be a more efficient drying agent than silica gel and anhydrous $CuSO_4$. The desolvated $Co^{II}(pybz)_2$ can absorb several gases such as CO_2, N_2, H_2, and CH_4 and also vapors of methanol, ethanol, benzene, and cyclohexane. If $Co^{II}(pybz)_2$ is exposed to air and followed by reactivation, its sorption capacity is considerably reduced, which we associate with a poisoning effect. Because of the long distance between the cobalt atoms in the structure, the magnetic properties are those of a paramagnet.

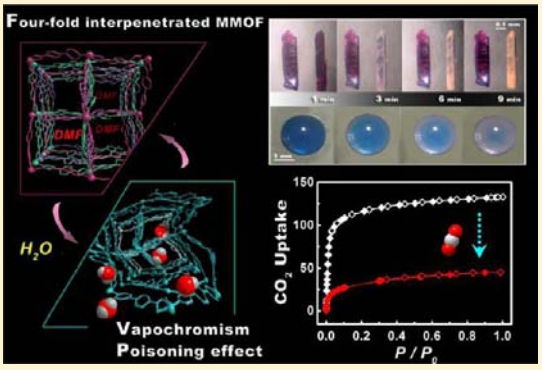

INTRODUCTION

The rapid development of metal−organic frameworks (MOFs) has led to active discussions of these materials as high prospects for potential applications in areas such as gas storage,[1] chemical sensing,[2,3] and separation.[4] Because "nature abhors a vacuum and interpenetration reduces voids", it is believed that enhanced porosity and high internal surface area are counterintuitive to the presence of interpenetrating lattices.[5] Among the most important types of interpenetrating topologies is the diamond network, usually constructed of four tetrahedrally divergent linear ditopic linkers.[6] They may have "self-recognition" characteristics, and depending on the length of the linker, they generate high-fold interpenetrating lattices (larger than three) to avoid the formation of large open channels or cavities.[5,7] Among the observed interpenetrated lattices, high-fold interpenetrating diamond networks constructed of linear ligands and displaying porosity are rare.[8,9] However, those formed by four-connective ligands displaying 1D channels and strain at the metal centers because of torsion and distortion of the ligands are rarer.[8] These systems may force the entire skeleton in a tight geometry, thus creating unusual properties. In this regard, the above porous networks may contain potential or strain energy and undergo changes in structure and properties with the release of that energy in response to a specific stimulus.[2,10] Appropriate external stimuli can perturb the coordination sites of the network and its connectivity by inducing the breaking and making of bonds.[11−13] Such a system offers us an experimentally unexplored field to study and expand the intermediate subtle region between *robustness and flexibility* through dynamic single-crystal-to-single-crystal (SCSC) and/or solid transformations.[12−14] If there are strong interactions within or between each framework, a domino reaction may follow and can result in unexpected physical and chemical phenomena.[15] Such solids make up an interesting and potentially useful class of "semisoft porous crystals", and they offer the opportunity to develop new materials with properties vastly different from

Received: August 24, 2012
Published: February 11, 2013

   dx.doi.org/10.1021/ic301857h | *Inorg. Chem.* 2013, 52, 2353−2360

those currently available.[10,13] Herein we report a 4-fold-interpenetrated diamond network, $[Co(pybz)_2]\cdot 2DMF$ [**1**·2DMF; $pybz^-$ = 4-(4-pyridyl)benzoate anion], and its unusual features: chromism upon multiple bond breaking, strained networks containing potential energy and strain, "domino effect" of structural relaxation, crystalline, and solid structure transformations, and selective gas adsorption under different stimuli as well as a poisoning effect.

EXPERIMENTAL SECTION

Synthesis of the Compounds. 4-(4-Pyridyl)benzoic acid was prepared as described in the literature,[16] and all solvents and other chemicals of standard grade were used as received. **1**·2DMF (where DMF = *N*,*N*-dimethylformamide) was prepared by the following procedure. A mixture of $Co(NO_3)_2\cdot 6H_2O$ (0.5 mmol), 4-(4-pyridyl)-benzoic acid (1.0 mmol), and DMF (15 mL) was stirred for 10 min in air. The product was placed in a 23-mL Teflon-lined autoclave and heated at 383 K for 48 h. The autoclave was cooled over a period of 11 h at a rate of 10 K/h, and claret-red crystals of **1**·2DMF were collected and washed with dried DMF. Yield: 65% (based on Co).

The desolvated **1** was obtained by two different approaches: one way was by heating **1**·2DMF in air at 423 K for 2 h, and the second way was by heating the methanol-loaded crystals at 355 K for 1 h. Methanol-exchanged sample **1**·4MeOH was obtained by soaking the crystals of as-prepared **1**·2DMF in dried methanol for 2 days with renewal of methanol several times at room temperature. Methanol replaces DMF easily after a few hours. It can also be obtained by placing the desolvated crystals in an atmosphere of methanol vapor or just soaking them in dried methanol. Ethanol-exchanged sample **1**·2.5EtOH was obtained using the same procedure as that of **1**·4MeOH but using dried ethanol instead. In addition, cyclohexane- and benzene-loaded crystals **1**·*x*guest (guest = C_6H_{12} or C_6H_6) were obtained using similar procedures by soaking desolvated crystals in dried cyclohexane and benzene.

X-ray Crystallography. Diffraction intensities of all compounds were collected on a Bruker Apex CCD area-detector diffractometer (Mo Kα, λ = 0.71073 Å). Absorption corrections were applied by using the multiscan program *SADABS*.[17] The structures were solved by direct methods and refined with a full-matrix least-squares technique within the *SHELXTL* program package.[18] All non-hydrogen atoms were refined with anisotropic displacement parameters. The organic hydrogen atoms were generated geometrically (C–H 0.96 Å), except for parts of the solvent molecules. The disordered guest DMF molecules for **1**·2DMF cannot be modeled and were treated by the *SQUEEZE* routine of *PLATON*.[19] For all structures, the amount of guest molecules were determined by thermogravimetric analysis (TGA) results. The crystal data and structure refinement results are listed in Table S1 in the Supporting Information (SI), while the selected bond distances and bond angles are listed in Tables S2–S5 in the SI. The CCDC reference numbers are 875175–875178 for **1**·2DMF, **1**, **1**·4MeOH, and **1**·2.5EtOH, respectively. The supplementary crystallographic data for these compounds can be found in the SI or can be obtained free of charge from the Cambridge Crystallographic Data Centre via http://www.ccdc.cam.ac.uk/data_request/cif.

Measurements Details. TGA was performed on a Netzsch TG 209 instrument in flowing N_2 with a heating rate of 10 °C/min. Powder X-ray diffraction (PXRD) measurements were performed on a Bruker D8 ADVANCE X-ray diffractometer with Cu Kα radiation. For variable-temperature PXRD measurements, the patterns for different temperatures were recorded after the sample had been kept at the respective temperature for 10 min in flowing N_2. The crystalline powder samples were prepared by crushing the single crystals, and scans of 3–60° with a rate of 5°/min were recorded. Calculated patterns of **1** were generated using PowderCell. Raman spectra were obtained using a Renishaw inVia Raman microscope equipped with a 785-nm diode laser and a 1200 lines/mm grating. The calorimetric experiment was performed by using a Micro DSC III apparatus (SETARAM, France). The sorption isotherm for N_2 was measured with an automatic volumetric adsorption apparatus (IGA-003 series, Hiden Isochema Ltd.) at 77 K. The low-pressure sorption measurements were performed using a Belsorp-Max automatic volumetric adsorption apparatus. The high-pressure gas sorption measurements were performed using the Belsorp HP-60 high-pressure sorption system. The magnetic susceptibility data of random-orientation powder samples were collected in the temperature range of 2.0–300 K with a Quantum Design MPMS XL-5 SQUID magnetometer.

RESULTS AND DISCUSSION

1·2DMF contains all three components of the solvothermal reaction: the linear rigid bifunctional ligand $pybz^-$, the cobalt atom as the node of the primary building unit, and DMF of the solvent used. X-ray crystallography reveals that **1**·2DMF crystallized in the chiral space group $P4_12_12$. Each cobalt(II) center adopts a distorted octahedral geometry by coordinating to two pyridine nitrogen atoms and two highly strained chelating carboxylate groups of $pybz^-$ (Figure 1a). The Co–N

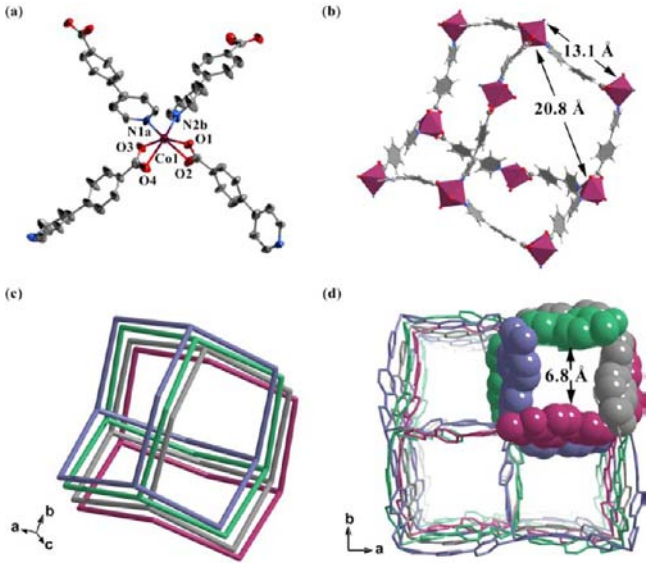

Figure 1. (a) Coordination environment of Co^{2+} ions in **1**·2DMF. General color code: Co, plum; N, blue; O, red; C, gray (50% probability ellipsoid; hydrogen atoms are not shown for clarity). (b) Perspective view of the diamondoid network of a single cobalt node connected by four organic linkers. (c) Schematic of the 4-fold-interpenetrated framework. (d) Perspective views of the 3D open framework with 1D channels in **1**·2DMF. The guest DMF molecules occupying the channels are not shown.

distances [2.065(4) and 2.077(4) Å] and the N–Co–N angle [100.3(2)°] are normal, but the Co–O distances [2.264(3) and 2.280(3) Å] are long and the chelating O–Co–O angles [59.9(1)° and 60.3(1)°] are narrow because of the high strain imposed by the chelating carboxylate. Thus, the cobalt coordination is highly distorted.[8,16] For the two $pybz^-$ groups, the dihedral angles between the pyridine and phenyl rings are 9.03(4)° and 31.11(7)°, and those of the O–Co–O–C and phenyl rings are 7.43(6)° and 28.60(5)°, respectively. If the chelating carboxylates are treated as one connecting arm, each cobalt(II) center has a pseudotetrahedral geometry with four divergent ligands that are connected to four other cobalt(II) centers in a tetrahedral fashion with an average core angle of 110°. This results in a diamondoid network of single-atom node of cobalt connected by the long organic ligand, where the Co···Co edges are about 13.1 Å. The maximum dimension of

dx.doi.org/10.1021/ic301857h | *Inorg. Chem.* 2013, 52, 2353–2360

Table 1. Comparsion of the Torsional Angles (deg) of the Aryl Rings and Carboxyl Groups among 1·2DMF, 1, 1·4MeOH, and 1·2.5EtOH[a]

	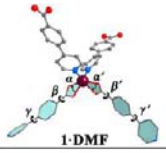 1·DMF	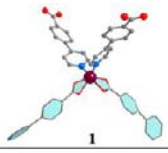 1	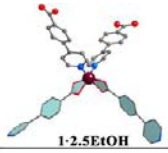 1·2.5EtOH	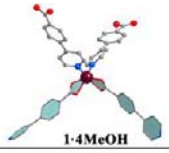 1·4MeOH	Max. deviation (%)
α'	59.91(4)	61.01(1)	60.30(3)	60.30(2)	1.8
α'	60.28(1)	60.14(1)	60.31(3)	60.57(2)	0.7
β	7.43(6)	6.30(5)	9.42(2)	6.87(1)	49.5
β'	28.60(5)	29.43(5)	27.61(1)	27.73(8)	6.6
γ	9.03(4)	8.59(4)	9.72(9)	8.84(6)	13.2
γ'	31.11(7)	32.51(6)	29.99(1)	31.76(8)	8.4

[a]The maximum deviation was calculated by the maximum difference of the angle divided by the minimum angle.

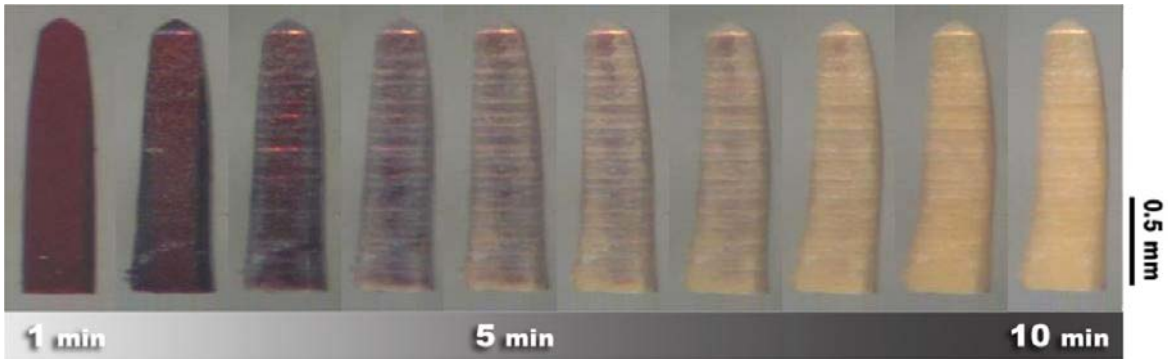

Figure 2. Time evolution of a crystal of **1**·2DMF undergoing a color change in 65% humidity.

open space of a single network is about 20.8 Å (Figure 1b), which would be unstable.[5]

Consequently, the structure is stabilized by a 4-fold interpenetration of the networks (Figure 1c), with an interpenetration vector running along the *c* axis. There are moderate-strength hydrogen bonds,[19] C−H···O in the range of 3.382(1)−3.609(1) Å, and an angle range of 143.5(6)−149.2(6)°, between adjacent diamondoid lattices (Figure S1 in the SI), which are different from the typical interpenetrating diamondoid nets and give considerable stability to the overall structure. The hydrogen bonds effectively prevent relative motion of each diamondoid net and are among the main factors responsible for its robustness.[16] Despite the 4-fold interpenetration, the arrangement of $pybz^-$ ligands is compact in the *a* and *b* directions and O1 and O4A have C−H···O interaction with the pyridine and phenyl rings, which generates 1D square-sectioned channels along the *c* axis, with a window size of 6.8 × 6.8 Å (Figures 1d and S2 in the SI). The *PLATON*-calculated void volume (V_{void}) of **1**·2DMF without guest DMF molecules is 47%.[20] There are some examples in which open structures result despite the high-fold interpenetration, and they sometimes provide very robust porous solids.[8,21]

X-ray diffraction (XRD) studies of the desolvated crystals were first attempted on crystals of **1**·2DMF heated at 423 K. These studies were not fully successful because of the large mosaicity and the high thermal motion at this high temperature. The structure was finally obtained on a crystal treated in the following way. Freshly prepared crystals of **1**·2DMF were soaked in dry MeOH, where the latter replaces DMF. Then one of the crystals was studied by XRD at 355(2) K, after an initial mounting at 293 K and slow warming (50 K/h) in a stream of dry N_2. The crystal was allowed to equilibrate at 355(2) K for 5 h before full data sets were collected. The desolvated crystal showed no perceptible change in appearance. The high-temperature structure of **1** confirms that the total removal of all of the guest molecules was achieved without loss of crystallinity. The very low residual electron density indicates that no MeOH remains in the channels. The framework retains all of the connectivity of the original structure with only slight changes in the metal−ligand bond distances and angles (Table S3 in the SI). This result really demonstrates the existence of porosity in this framework.

For solvent-exchanged crystals, the single-crystal data analyses reveal that **1**·4MeOH and **1**·2.5EtOH also crystallize in the space group $P42_12$ and maintain the 3D frameworks with 1D channels but the torsion angles partly changed (Table 1). It is interesting to note that the framework with the inclusion of these two alcohols appears to be more stable than **1**·2DMF. This is further evidenced by these two compounds having unit cell volumes less than (methanol) or equal to (ethanol) that of the solvent-free compound, indicating strong solvent−framework interaction.

In fact, long Co−O bonds, 4-fold interpenetrating frameworks, hydrogen bonds between adjacent diamond cages, and relative dihedral motion of the aryl rings and carboxyl groups are all present as in the original structure with DMF. These support the entire skeleton in a tight and robust state, which retains the potential or strain energy and undergoes changes in the structure and property in response to a specific stimulus (such as thermal desolvation or solvent inclusion), involving

dx.doi.org/10.1021/ic301857h | *Inorg. Chem.* 2013, 52, 2353−2360

the breaking of several bonds.[10,11] It is quite surprising that the polar alcohols do not remove the strain of the chelating carboxylate group. We associate this with geometric constraints around the cobalt coordination sphere.

Interestingly, single crystals of **1**·2DMF standing in air at ambient temperature for 10 min undergo a rapid transformation to yield compound $Co(pybz)_2 \cdot xH_2O \cdot y$DMF (**1′**). The process is accompanied by a color change from claret red to pink, distortion of the crystal shape, and loss of crystallinity (Figure 2).

The vapochromism can be ascribed to the change of the geometry from a very strained octahedron imposed by the two chelating carboxylate groups to a more relaxed octahedron due to the coordination of water molecules transforming the two chelating carboxylate groups to monodentate: thus, a change in the ligand-field energies of the d orbital of cobalt(II) to the common pink color of a regular octahedral cobalt(II). Raman spectra confirm this conclusion, where the carboxylate mode from μ_1-κ-O,O′ to μ_1-κ-O is identified (Figure S3 in the SI).[22] The mechanism proposed is that water from the atmosphere relieves the strain at the cobalt site by breaking one of the chelating Co−O (carboxylate) bonds near the windows at the channel of the 4-fold-interpenetrated diamondoid networks, and this then replaces DMF progressively through the rest of the crystals. If the initial step is preferentially on one surface, then it will progress through the crystal to the other side. This may be the reason for the crystal being curved during the process.[23] Accompanying the change in the coordination geometry at the cobalt center, the $pybz^-$ ligands become coplanar through the rotation of aryl rings, the thus less occupied pore, as well as relaxation and relative motion of each diamondoid network. As a result, the shrinkage of 1D channels is unavoidable. This finding shows a way to release the potential energy or strain stored up by a tight framework or partially serious distortion of a strained coordination geometry system.[10,11]

However, the crystal diffraction power of the pink crystal **1′** is too low to determine the structure. It is to be noted that the shape is modified from being straight to having a slight curvature (Figure 2). This is often the case when hydration or dehydration occurs preferentially from one surface.[23] This could be the cause for the low diffracting power.

The exact solvent content of **1′** is difficult to estimate because of the departure of DMF at fairly low temperature. We tried another way to estimate the water content by measuring the water absorption isotherms of desolvated **1** followed by TGA on the same batch of crystals. The desolvated phase of **1** was placed on an electronic analytical balance having a precision of 10^{-6} g and allowed to adsorb water in air under a humidity of 60% at 27 °C (Figure S4 in the SI). The adsorption takes place rapidly in the first 20 min to a plateau corresponding to **1**·$3H_2O$ and then slowly approaches saturation with an amount of 171 mg of H_2O adsorbed per 1 g of compound. The adsorption at saturation is equivalent to 4.5 molecules of water per formula unit, that is, **1**·$4.5H_2O$. This is in good agreement with the measurement of TGA (Figure S5 in the SI).

From the four structures determined and the effect of moisture on the crystals of **1**·2DMF as well as **1**, we can conclude that DMF, methanol, and ethanol are not able to coordinate to the cobalt centers because of the lack of space available for these solvents to get near the cobalt(II) ion. However, it appears that only the water molecule is able to reach the fairly tight space and coordinate to the cobalt atoms. To the best of our knowledge, this particular observation is unique to this compound.[8,11,24] For this reason, water displays a poisoning effect (see later). We should note also that from the gas sorption experiments only methanol is able to remove the coordinated water (see later).

Further, the process of desolvation of the as-prepared red compound **1**·2DMF to **1** in an inert atmosphere is rather slow to achieve completeness. The crystals retain the red coloration after the process. This may indicate that the geometry around the cobalt atom is not so perturbed. Water molecules may then attack the cobalt sites more easily to relieve the strain by breaking one of the Co−O bonds (Co−O1 and Co−O4A) of the chelating carboxylate group. Surprisingly, the water absorption appears to be easier for **1**·2DMF than for **1** (Figure S6 in the SI). Thus, it appears that water can reach the metal easier when DMF is in the channel. We may then assume that the space around the metal is more easily accessible when DMF is present than when it is absent. However, after exposure of **1** in air for about 90 min, it also changes from the initial red to pink (Figure S6 in the SI).

To examine the thermal stability of the porous 4-fold-interpenetrated diamond network, TGA and PXRD measurements were carried out as a function of the temperature. The TGA curve (Figure S7 in the SI) of **1**·2DMF shows that the solvent DMF molecules can be removed at 220 °C to give the empty microporous **1**. The PXRD patterns of **1**·2DMF were recorded in the range of 25−500 °C under a N_2 atmosphere (Figure S8 in the SI). It is clear that the diffraction profiles below 320 °C are almost the same, indicating that the microporous framework is stable up to this temperature and the crystal retains the framework structure after removal of the guest DMF molecules. It can be concluded that **1** has excellent thermal stability in the class of MOFs under a dry environment.[14]

Furthermore, the in situ PXRD pattern of **1**·2DMF exposed in air was measured to follow the color change process (Figure 3). It is clear that only the [400] reflection shifts to lower 2θ values, which is consistent with constriction of the 1D channels.[25] The other reflections gradually weakened because the structural changes during the process readily caused a loss of crystallinity.

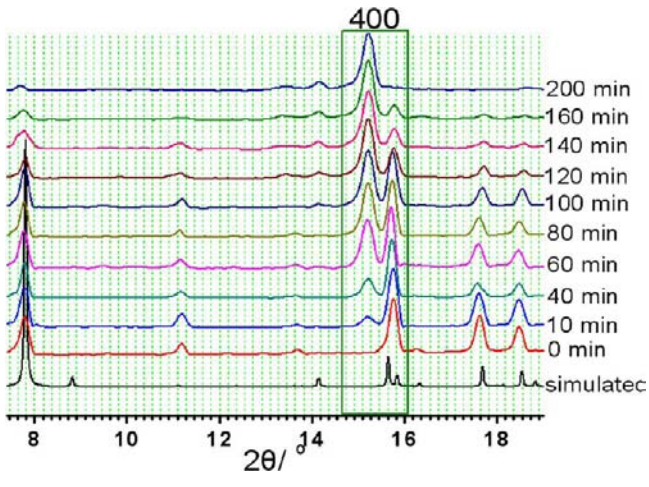

Figure 3. Time dependence of PXRD of **1**·2DMF in air at room temperature.

dx.doi.org/10.1021/ic301857h | *Inorg. Chem.* 2013, 52, 2353−2360

On the other hand, Raman spectra of **1**·2DMF and **1**·4.5H_2O have been analyzed to understand the change of the cobalt(II) coordination environment and coordination mode of the carboxyl group (Figure S3 in the SI). The COO^- symmetric stretching of **1**·2DMF and **1**·4.5H_2O appears at 1416 and 1388 cm^{-1}, respectively, with the absence of any shoulder or incidental scattering.[22] The shift of 28 cm^{-1} of **1**·4.5H_2O to lower wavelength suggests that the symmetry of COO^- changed evidently. More importantly, the moderate peak at 409 cm^{-1} for **1**·2DMF, which was assigned to the vibration of Co−O coordination bonds, splits into 413 and 392 cm^{-1}, indicating that the $pybz^-$ carboxylate groups function in two different coordination fashions and suggesting that the coordination mode of the carboxyl group has changed from μ_1-κ-O,O′ to μ_1-κ-O during the solid structural transformation.[22] Meanwhile, 1520 cm^{-1} is assigned to the C═O stretching of each complex, and the intensity of the C═O stretching mode of **1**·4.5H_2O is stronger than that of **1**·2DMF because the character of C═O obviously boosts when **1**·2DMF changes to **1**·4.5H_2O. The above analysis is in agreement with our hypothesis.

The molar enthalpies of the solid−liquid of guest exchange and inclusion processes in **1**·2DMF by the microcalorimetric method have been studied (Figure S9 in the SI). The large and negative sign of the molar enthalpy ΔH_θ^m of −66.63 kJ/mol indicates that the solid−water reaction is radical.[26] The apparent energy of the reaction indicates that the $pybz^-$ groups, which are twisted in the as-synthesized material, return to the coplanar state and release the strain produced from the twist in the $pybz^-$ groups and 4-fold-interpenetrated framework.

Several materials, for example, silica gel and bluestone, can rapidly display a color change when in contact with water. When exposed to dry air, they will take a long time to change color. In comparison, **1**·2DMF not only possesses all of the strong points of these materials but also possesses some other additional characteristics. **1**·2DMF, which does not dissolve in water and most common solvents, can rapidly change color in only a few minutes when exposed to air, bearing a comparison with silica gel and being much quicker than anhydrous $CuSO_4$ (Figures 4 and 5). Recently, several compounds that change color via single-crystal-to-single-crystal or solid transformation have been reported,[11,26b,27] but none of these compounds are as sensitive as **1**·2DMF to water. Therefore, **1**·2DMF may be the most appropriate candidate as a new-fashioned water indicator.[2]

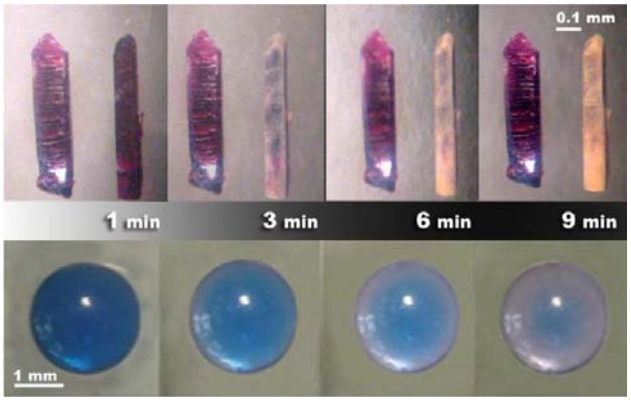

Figure 4. Comparison of the color changes for **1** (left), **1**·2DMF (right), and a silica gel (below) under a 65% humidity atmosphere at 30 °C.

In order to compare the structure transformation and the change of channels of as-synthesized and water-induced mutation, the sorption properties of **1** and **1a**, obtained separately by the desolvation of **1**·2DMF and **1**·4.5H_2O, respectively, have been performed with different gases (N_2, CO_2, H_2, and CH_4) as well as various volatile organic solvents (methanol, ethanol, benzene, and cyclohexane) as combustible molecules.

The CO_2 gas sorption isotherms for **1** at 195 K show a typical type I behavior characterized by a plateau reaching a saturated adsorptive capacity of 133 cm^3/g at low relative pressure (Figure 6). This early uptake indicates the presence of permanent microporosity in **1**, and a Langmuir surface area of 770 m^2/g was obtained by fitting the sorption curve (Figure S10 in the SI). This value is uncompetitive with those reported for high-surface-area 3D PCPs,[28] but it is comparable to those reported for MOFs with 1D channels and outstanding among the high-fold interpenetration MOFs.[14a,29] However, being different from CO_2 gas sorption isotherms, the desolvated sample has nearly no N_2 sorption at all, similar to some MOFks with large pores but exhibiting no sorption of nitrogen at 77 K (Figure S11 in the SI).[30]

In contrast, although **1a** also shows a type I CO_2 sorption curve at 195 K (Figure 6), the saturated adsorptive capacity is lowered to 44 cm^3/g, which corresponds to a Langmuir surface area of just 261 m^2/g (Figure S12 in the SI). Understandably, **1a** has no N_2 sorption as well. Obviously, both **1** and **1a** exhibit selective sorption of CO_2 over N_2 because nearly no sorption of N_2 was observed. More importantly, this undoubtedly confirms that the tight skeleton is rather stable even after the removal of guest molecules which differ from easily collapsed first-generation MOFs.[31] However, the perturbation of water molecules induced the release of potential tension and shrinking channels, while the network connectivity is maintained.[23]

There have been some reports of gate-opening phenomenon in flexible MOFs.[32] Can high pressure help the recovery of the shrinking channels of **1a**? So, the high-pressure H_2 and CH_4 gas sorption behaviors of **1** and **1a** were studied. The H_2 (at 77 K) and CH_4 (at 298 K) uptake of **1** increased along with an increase of the pressure with a saturated uptake of about 212 cm^3/g for H_2 at 20 bar and about 95 cm^3/g for CH_4 at 35 bar (Figure 7). It should be noted that the H_2 uptake of 145 cm^3/g at 1.0 bar for **1** is high compared to those for other MOFs with 1D channels (Table S6 in the SI), which suggests strong hydrogen−framework interactions. The H_2 uptake of **1a** at 77 K also increased with pressure to 60 cm^3/g (about 30% of that of **1**) but remains unsaturated. However, there is no adsorption for **1a** to CH_4. So, the limited hydrogen sorption and no sorption of methane by **1a** is clear evidence that the pores are poisoned by water.

None of the gas molecules, CO_2, N_2, CH_4, and H_2, can restore the sorption behavior of **1a** to **1**.[33] So, we design a simple experiment by soaking **1** and **1a** in different organic solvents such as methanol, ethanol, benzene, and cyclohexane to compare their relative sorption abilities. TGA measurements (Figures 8 and S13 in the SI) show that the amounts of methanol, ethanol, benzene, and cyclohexane adsorbed by **1** were about 287, 254, 261, and 199 mg/g, respectively, which are equivalent to approximately 4 molecules of methanol, 2.5 molecules of ethanol, 1.5 molecules of benzene, and 1 molecule

dx.doi.org/10.1021/ic301857h | Inorg. Chem. 2013, 52, 2353−2360

Figure 5. Comparison of the color changes for **1**·2DMF (left) and $CuSO_4$ (right) under a 65% humidity atmosphere at 30 °C.

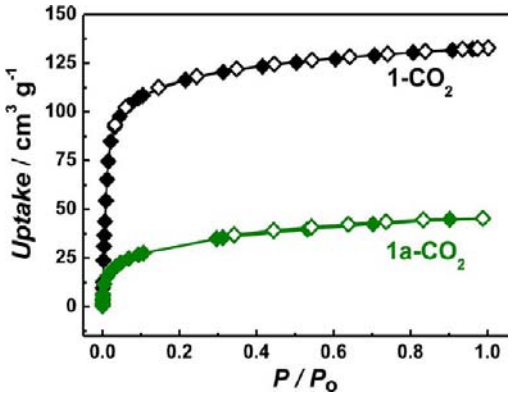

Figure 6. CO_2 (195 K) gas sorption isotherms for **1** and **1a**.

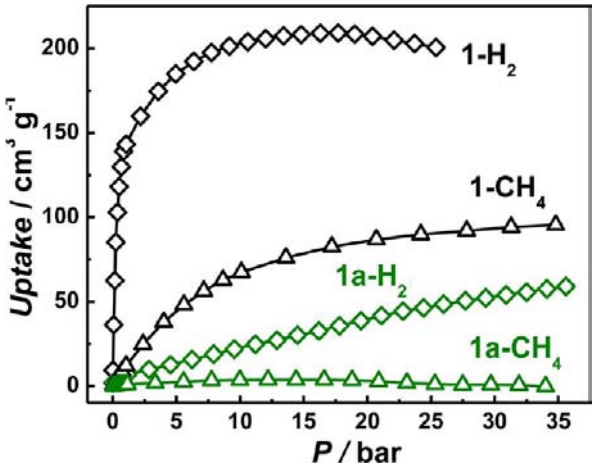

Figure 7. High-pressure H_2 (77 K) and CH_4 (298 K) gas sorption isotherms for **1** and **1a**.

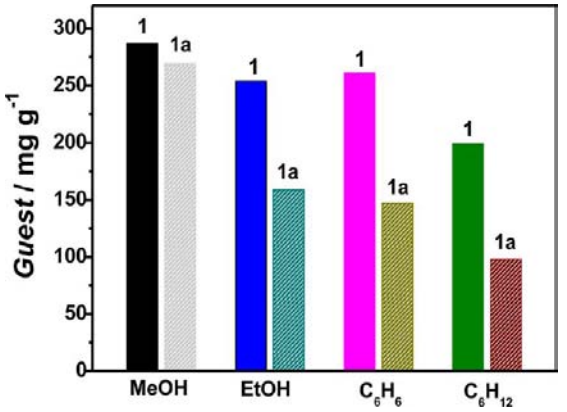

Figure 8. Comparison of the guest uptake for different volatile organic solvents of **1** and **1a**.

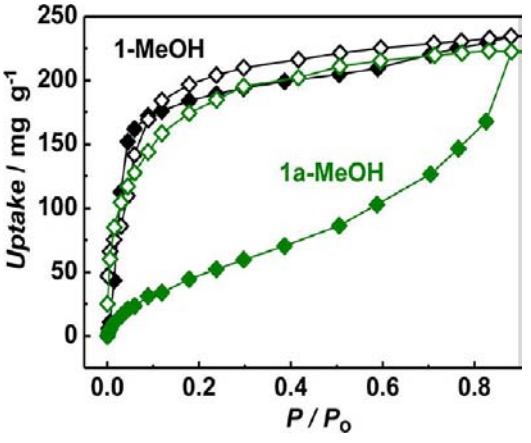

Figure 9. Methanol vapor sorption (298 K) isotherms for **1** and **1a**.

of cyclohexane per formula unit. In contrast, the sorption amounts of methanol, ethanol, benzene, and cyclohexane by **1a** are 269, 159, 147, and 98 mg/g, or 3.8, 1.7, 0.9, and 0.5 molecules per formula unit, respectively. Obviously, the adsorption amounts of ethanol, benzene, and cyclohexane of **1a** are evidently decreased (lost about 37−51%) compared to those of **1**. However, the MeOH adsorption amount of **1a** is nearly matched to that of **1** (lower by just about 6%). So, different organic solvents exhibited different restoring abilities for **1a**; especially, methanol can almost realize the complete recovery of the pores.

Furthermore, we measure the vapor sorption behavior of **1** and **1a** using methanol, benzene, and cyclohexane as candidates. As shown in Figure 9, the sorption of **1** for methanol shows rapid increases in the low-pressure range (P/P_0 < 0.2) and then slowly approaches saturation with the amount adsorbed of 234 mg/g at P/P_0 = 0.88. The desorption curve does not retrace the adsorption isotherm, showing partly hysteresis and incomplete desorption, while the sorption of **1a** for methanol shows a gradual increase with increasing P/P_0 and the amount adsorbed is 222 mg/g at P/P_0 = 0.88, which is just a little less than that of **1**. However, the desorption curve of **1a** is very similar to **1**. On the other hand, the sorption isotherms of benzene and cyclohexane vapors by **1a** at room temperature show typical type I shape with saturated sorption amounts of 178 and 86 mg/g, respectively (Figure S14 in the SI), which are lower than the sorption amounts of **1** in corresponding solvents (261 and 199 mg/g).

These results suggest that the pore opening of **1a** is, in fact, solvent-dependent. The small size of methanol molecules compared to ethanol, benzene, and cyclohexane permits them to easily enter the shrinking channels. Moreover, hydrogen interaction between methanol and the framework may be a

dx.doi.org/10.1021/ic301857h | Inorg. Chem. 2013, 52, 2353−2360

crucial factor concluded from the rapid increases of the methanol amounts in the low-pressure range (P/P_0 < 0.1) as well as the hysteretic desorption curve. Importantly, this is in good agreement with the presence of the strong solvent−framework interaction suggested by the unit cell volume. So, the shape, size, and host−guest interaction cooperatively affect the modulation and recovery of the framework and channel upon incorporation with different guest molecules.[32,33] This was also confirmed by the TGA measurements of **1** and **1a** after the sorption of different organic solvents because the uptake loss of **1a** compared to **1** obeys MeOH < EtOH < C_6H_6 < C_6H_{12} (Table S7 in the SI).

CONCLUSION

In summary, **1**·2DMF is a rare and vivid example showing the release of the potential energy or strain stored up by a tight framework or partially serious distortion of a strained molecular system for the first time when in contact with water vapor. It not only represents a significant new addition to the growing number in the flexible MOF family but also illustrates a new strategy to research flexible MOFs that are sensitive to small molecules by utilizing in situ XRD, Raman spectroscopy, microcalorimetry, and adsorption. In addition, **1**·2DMF may be the new type of water indicator because of its high sensitivity for water. Poisoning is presented and clearly demonstrated for the first time in MOFs.

ASSOCIATED CONTENT

Supporting Information

Addition files, synthesis, crystal data in CIF format, and IR, TGA, PXRD, and UV/vis spectral data. This material is available free of charge via the Internet at http://pubs.acs.org.

AUTHOR INFORMATION

Corresponding Author

*E-mail: zmh@mailbox.gxnu.edu.cn.

Notes

The authors declare no competing financial interest.

ACKNOWLEDGMENTS

This work was supported by the NSFC (Grants 91022015 and 91122032), GXNSFC (Grant 2010GXNSFF013001), Guangxi Province Science Funds for Distinguished Young Scientists (Grant 2012GXNSFFA060001), Project of Talents Highland of Guangxi Province, and Project of Talents Highland of Colleges and Universities in Guangxi Province. M.K. thanks the CNRS-France for funding.

REFERENCES

(1) (a) Rowsell, J. L. C.; Yaghi, O. M. *Angew. Chem., Int. Ed.* **2005**, *44*, 4670−4679. (b) Murray, L. J.; Dincă, M.; Long, J. R. *Chem. Soc. Rev.* **2009**, *38*, 1294−1314. (c) Suh, M. P.; Hye, J. P.; Prasad, T. K.; Lim, D. W. *Chem. Rev.* **2012**, *112*, 782−835. (d) Farha, O. K.; Yazaydin, O.; Eryazici, I.; Malliakas, C.; Hauser, B.; Kanatzidis, M. G.; Nguyen, S. T.; Snurr, R. Q.; Hupp, J. T. *Nat. Chem.* **2010**, *2*, 944−948.

(2) (a) Kreno, L. E.; Leong, K.; Farha, O. K.; Allendorf, M.; Duyne, R. P. V.; Hupp, J. T. *Chem. Rev.* **2012**, *112*, 1105−1125. (b) Lu, G.; Hupp, J. T. *J. Am. Chem. Soc.* **2010**, *132*, 7832−7833.

(3) (a) Pramanik, S.; Zheng, C.; Emge, T. J.; Li, J. *J. Am. Chem. Soc.* **2011**, *133*, 4153−4155. (b) Rosseinsky, M. J. *Nat. Mater.* **2010**, *9*, 609−610. (c) Lu, Z.-Z.; Zhang, R.; Li, Y.-Z.; Guo, Z.-J.; Zheng, H.-G. *J. Am. Chem. Soc.* **2011**, *133*, 4172−4174.

(4) (a) Li, J.-R.; Sculley, J.; Zhou, H.-C. *Chem. Rev.* **2012**, *112*, 869−932. (b) Bae, Y.-S.; Lee, C. Y.; Kim, K. C.; Farha, O. K.; Nickias, P.; Hupp, J. T.; Nguyen, S. T.; Snurr, R. Q. *Angew. Chem., Int. Ed.* **2012**, *51*, 1857. (c) Bloch, E. D.; Queen, W. L.; Krishna, R.; Zadrozny, J. M.; Brown, C. M.; Long, J. R. *Science* **2012**, *335*, 1606−1610. (d) Southon, P. D.; Price, D. J.; Nielsen, P. K.; McKenzie, C. J.; Kepert, C. J. *J. Am. Chem. Soc.* **2011**, *133*, 10885−10891.

(5) (a) Batten, S. R.; Robson, R. *Angew. Chem., Int. Ed.* **1998**, *37*, 1460−1494. (b) Batten, S. R. *CrystEngComm* **2001**, *18*, 1−7.

(6) (a) O'Keeffe, M.; Peskov, M. A.; Ramsden, S. J.; Yaghi, O. M. *Acc. Chem. Res.* **2008**, *41*, 1782−1729. (b) Tan, C.-R.; Yang, S.-H.; Champness, N. R.; Lin, X.-A.; Blake, A. J.; Lewis, W.; Schroder, M. *Chem. Commun.* **2011**, *47*, 4487−4489. (c) Zhang, J.; Bu, X.-H. *Angew. Chem., Int. Ed.* **2007**, *46*, 6115−6118.

(7) Wu, H.; Yang, J.; Su, Z.-M.; Batten, S. R.; Ma, J.-F. *J. Am. Chem. Soc.* **2011**, *133*, 11406−11409.

(8) Batten, S. R.; Neville, S. M.; Turner, D. R. *Coordination Polymers Design, Analysis and Application*; The Royal Society of Chemistry: London, 2009; pp 273−372.

(9) Ma, L.-Q.; Lin, W.-B. *Angew. Chem., Int. Ed.* **2009**, *48*, 3637−3640.

(10) Horike, S.; Shimomura, S.; Kitagawa, S. *Nat. Chem.* **2009**, *1*, 695−704.

(11) (a) Kawano, M.; Fujita, M. *Coord. Chem. Rev.* **2007**, 2592−2605. (b) Kitagawa, S.; Matsuda, R. *Coord. Chem. Rev.* **2007**, *251*, 2490−2509.

(12) (a) Maji, T. K.; Matsuda, R.; Kitagawa, S. *Nat. Mater.* **2007**, *6*, 142−148. (b) Park, H. J.; Lim, D.-W.; Yang, W. S.; Oh, T.-R.; Suh, M. P. *Chem.—Eur. J.* **2011**, *17*, 7251−7260.

(13) Yin, Z.; Zeng, M.-H. *Sci. China: Chem.* **2011**, *54*, 1371−1394 (review)..

(14) (a) Zeng, M.-H.; Wang, Q.-X.; Tan, Y.-X.; Hu, S.; Zhao, H.-X.; Long, L.-S.; Kurmoo, M. *J. Am. Chem. Soc.* **2010**, *132*, 2561−2563. (b) Chen, Q.; Lin, J.-B.; Xue, W.; Zeng, M.-H.; Chen, X.-M. *Inorg. Chem.* **2011**, *50*, 2321−2328. (c) Jiang, Y.-M.; Yin, Z.; He, K.-H.; Zeng, M.-H.; Kurmoo, M. *Inorg. Chem.* **2011**, *50*, 2329−2333. (d) Hu, S.; He, K.-H.; Zeng, M.-H.; Zou, H.-H.; Jiang, Y.-M. *Inorg. Chem.* **2008**, *47*, 5218−5224. (e) Zeng, M.-H.; Wang, B.; Wang, X.-Y.; Zhang, W.-X.; Chen, X.-M.; Gao, S. *Inorg. Chem.* **2006**, *45*, 7069−7076. (f) Zeng, M.-H.; Feng, X.-L.; Zhang, W.-X.; Chen, X.-M. *Dalton Trans.* **2004**, 2217−2223.

(15) Chang, T. C. *Phys. Rev. Lett.* **2008**, *101*, 175501−175504.

(16) (a) Yin, Z.; Wang, Q.-X.; Zeng, M.-H. *J. Am. Chem. Soc.* **2012**, *134*, 4857−4863. (b) Evans, O. R.; Lin, W.-B. *Chem. Mater.* **2001**, *13*, 2705−2712.

(17) Sheldrick, G. M. *SADABS 2.05*; University of Göttingen: Göttingen, Germany.

(18) *SHELXTL 6.10*; Bruker Analytical Instrumentation: Madison, WI, 2000.

(19) (a) Desiraju, G. R. *Acc. Chem. Res.* **1996**, *29*, 441−449. (b) Steiner, T. *Angew. Chem., Int. Ed.* **2002**, *41*, 48−76. (c) Jeffrey, G. A. *An Introduction to Hydrogen Bond*; Oxford University Press: New York, 1997.

(20) Spek, A. L. *J. Appl. Crystallogr.* **2003**, *36*, 7−13.

(21) Kesanli, B.; Cui, Y.; Smith, M. R.; Bittner, E. W.; Brockrath, B. C.; Lin, W.-B. *Angew. Chem., Int. Ed.* **2005**, *44*, 72−75.

(22) (a) Nakamoto, K. *Infrared and Raman Spectra of Inorganic and Coordination Compounds*; John Wiley and Sons: New York, 2009; pp 1−222. (b) Zeng, M.-H.; Tan, Y.-X. et al. Unpublished results.

(23) Férey, G.; Serre, C. *Chem. Soc. Rev.* **2009**, *38*, 1380−1399.

(24) (a) Rabone, J.; Yue, Y. F.; Chong, S. Y.; Stylianou, K. C.; Bacsa, J.; Bradshaw, D.; Darling, G. R.; Berry, N. G.; Khimyak, Y. Z.; Ganin, A. Y.; Wiper, P.; Claridge, J. B.; Rosseinsky, M. J. *Science* **2010**, *329*, 1053−1057. (b) Guillou, N.; Millange, F.; Walton, R. I. *Chem. Commun.* **2011**, *47*, 713−715.

(25) Volkringer, C.; Loiseau, T.; Guillou, N.; Férey, G.; Elkaïmc, E.; Vimont, A. *Dalton Trans.* **2009**, 2241−2249.

(26) (a) Rosenbach, N.; Ghoufi, A.; Déroche, I.; Llewellyn, P. L.; Devic, T.; Bourrelly, S.; Serre, C.; Férey, G.; Maurin, G. *Phys. Chem.*

Chem. Phys. **2010**, *12*, 6428−6437. (b) Zeng, M.-H.; Hu, S.; Chen, Q.; Xie, G.; Shuai, Q.; Gao, S.-L.; Tang, L.-Y. *Inorg. Chem.* **2009**, *48*, 7070−7079.

(27) (a) Takaoka, K.; Kawano, M.; Tominaga, M.; Fujita, M. *Angew. Chem., Int. Ed.* **2005**, *44*, 2151−2154. (b) Haneda, T.; Kawano, M.; Kojima, T.; Fujita, M. *Angew. Chem., Int. Ed.* **2007**, *46*, 6643−6645. (c) Cheng, X.-N.; Zhang, W.-X.; Lin, Y.-Y.; Zheng, Y.-Z.; Chen, X.-M. *Adv. Mater.* **2007**, *19*, 1494−1498. (d) Armentano, D.; Munno, G. D.; Mastropietro, T. F.; Julve, M.; Lloret, F. *J. Am. Chem. Soc.* **2005**, *127*, 10778−10779. (e) Lee, E. Y.; Suh, M. P. *Angew. Chem., Int. Ed.* **2004**, *43*, 2798−2801.

(28) (a) Furukawa, H.; Ko, N.; Go, Y. B.; Aratani, N.; Choi, S. B.; Choi, E.; Yazaydin, A. O.; Snurr, R. Q.; O'Keeffe, M.; Kim, J.; Yaghi, O. M. *Science* **2010**, *239*, 424−428. (b) Zhang, Y.-B.; Zhou, H.-L.; Lin, R.-B.; Zhang, C.; Lin, J.-B.; Zhang, J.-P.; Chen, X.-M. *Nat. Commun.* **2011**, *3* (642), 1−9.

(29) (a) Li, Y.-W.; Wang, L.-F.; He, K.-H.; Chen, Q.; Bu, X.-H. *Dalton Trans.* **2011**, *40*, 10319−10321. (b) Zhang, Z.-J.; Xiang, S.-C.; Chen, Y.-S.; Ma, S.-Q.; Lee, Y.-W.; Phely-Bobin, T.; Chen, B.-L. *Inorg. Chem.* **2010**, *49*, 8444−8448. (c) Xu, J.; Bai, Z.-S.; Chen, M.-S.; Su, Z.; Chen, S.-S.; Sun, W.-Y. *CrystEngComm* **2009**, *11*, 2728−2733.

(30) (a) Vaidhyanathan, R.; Bradshaw, D.; Rebilly, J.-N.; Barrio, J. P.; Gould, J. A.; Berry, N. G.; Rosseinsky, M. J. *Angew. Chem., Int. Ed.* **2006**, *45*, 6495−6499. (b) Fletcher, A. J.; Cussen, E. J.; Prior, T. J.; Rosseinsky, M. J.; Kepert, C. J.; Thomas, K. M. *J. Am. Chem. Soc.* **2001**, *123*, 10001−10011.

(31) (a) Kitagawa, S.; Kondo, M. *Bull. Chem. Soc. Jpn.* **1998**, *71*, 1739−1753. (b) Kitagawa, S.; Kitaura, R.; Noro, S. *Angew. Chem., Int. Ed.* **2004**, *43*, 2334−2375.

(32) (a) Gücüyener, C.; Bergh, J. V. D.; Gascon, J.; Kapteijn, F. *J. Am. Chem. Soc.* **2010**, *132*, 17704−17706. (b) Tanaka, D.; Nakagawa, K.; Higuchi, M.; Horike, S.; Kubota, Y.; Kobayashi, T. C.; Takata, M.; Kitagawa, S. *Angew. Chem., Int. Ed.* **2008**, *47*, 3914−3918. (c) Cheng, Y.; Kajiro, H.; Noguchi, H.; Kondo, A.; Ohba, T.; Hattori, Y.; Kaneko, K.; Kanoh, H. *Langmuir* **2011**, *27*, 6905−6909.

(33) (a) Seo, J.; Matsuda, R.; Sakamoto, H.; Bonneau, C.; Kitagawa, S. *J. Am. Chem. Soc.* **2009**, *131*, 12792−12800. (b) Li, C.-P.; Du, M. *Chem. Commun.* **2011**, *47*, 5958−5972. (c) Demessence, A.; Long, J. R. *Chem.—Eur. J.* **2010**, *16*, 5902−5908.